



INFLUENCE OF GROUND IMPEDANCE ON THE SOUND RADIATION OF A RAILWAY TRACK

Xianying Zhang, David Thompson, Giacomo Squicciarini

ISVR, University of Southampton, Southampton SO17 1BJ, UK

e-mail: xz24g12@soton.ac.uk

Railway rolling noise is radiated by the vibration of the rail and wheel. The TWINS model is well established as a method of predicting the generation of vibration and noise and this has been used successfully to design noise mitigation measures. However, the existing model used to predict the sound radiation from the rail considers the rail to be located in free space whereas, in reality, the rail is attached to sleepers or is located above the ballast or slab. Therefore it is necessary to take these boundary conditions into account in order to propose more realistic models. In this paper, boundary element method calculations are carried out to investigate the influence of the ground in close proximity to the rail on the sound radiation from both vertical and horizontal motion of the rail. Ground absorption is introduced using the Delany-Bazley model for the acoustic impedance and its effect on the sound radiation is shown. The results are verified by experimental results obtained using a 1/5 scale model with different kinds of ground impedance.

1. Introduction

The most important source of environmental noise from railways is rolling noise. It is produced by track and wheel vibration, which is induced by the roughness at the wheel/rail contact area. The relative importance of the wheel and track radiation depends on details of the design, the roughness spectra and the train speed^{1,2}. Nonetheless, the component of noise radiated by the rail is often the highest. It is therefore necessary to understand the mechanisms of sound radiation by railway track in order to implement effective noise control measures.

The sound radiation from the rail was studied by Bender and Remington^{3,4}, with the assumption that the rail radiates as a cylinder into a free field. Practically, however, the rail is located on sleepers or above the ballast. Later, Remington⁵ improved the model, including the ground as a finite impedance plane using the approach of Chessell⁶. Comparison of analytical results and field measurements of radiated sound showed that the effects of the ground impedance, such as the absorptive ballast, should be included in future models.

Thompson extended the engineering methods for predicting rolling noise implementing them in a software package, known as TWINS ('Track-Wheel Interaction Noise Software')⁷. This prediction model for rolling noise is widely used in the railway industry and has been validated against experimental data. However, the rail radiation is predicted in the software using a two-dimensional model in free space, see also Ref. 1. To improve the predictions it is necessary therefore to include the effects of the ground in close proximity to the rail on the sound radiation of the rail.

This paper investigates the characteristics of the sound radiation by a rail when it is in free space, on a rigid ground and above a rigid ground, using boundary element calculations. Moreover,

the influence of an absorptive ground, defined by its impedance, on the sound radiation is presented. Finally, measurements are performed to verify the calculations.

2. Sound radiation of the rail

The radiation ratio of a vibrating structure can be written as

$$\sigma = \frac{W}{\rho_0 c_0 S \langle v^2 \rangle} \quad (1)$$

where ρ_0, c_0 are the density of the air and the speed of sound, respectively, W is the radiated sound power of the structure, S is the total surface area and $\langle v^2 \rangle$ is the surface-averaged mean-square normal velocity. The quantities σ , W and v are functions of frequency.

The geometry of a rail can be considered as two-dimensional, with the third dimension being infinite. As the wavelength of rail vibration is generally large compared with the acoustic wavelength, the radiated sound field can also be approximated as two-dimensional, allowing it to be calculated using a two-dimensional boundary element model. The validity of such an approach has been considered in Ref. 8 and shown to be valid in practical situations above about 250 Hz.

The sound radiation for a UIC60 rail is investigated here using a two-dimensional boundary element model based on the direct BEM approach. Three cases are considered, as shown in Figure 1. As well as a rail in free field, these are a rail attached to a rigid surface, such as a sleeper, and a rail at a certain distance above the surface, which can be considered to represent the condition above the ballast, although initially it is considered to be rigid. In the latter case, the sound radiation of the rail depends on the distance from the ground. A distance of 0.02 m is used in the present calculations. In all the calculations it is assumed, for simplicity, that the rail vibrates with a rigid body motion either vertically or horizontally.

In order to include the ground in the model, a rigid box is included beneath the rail with dimensions chosen large enough that the edges have no effect on the results. Two different models are used for low and high frequencies. CHIEF points are included inside the BE mesh to avoid problems at singular frequencies.

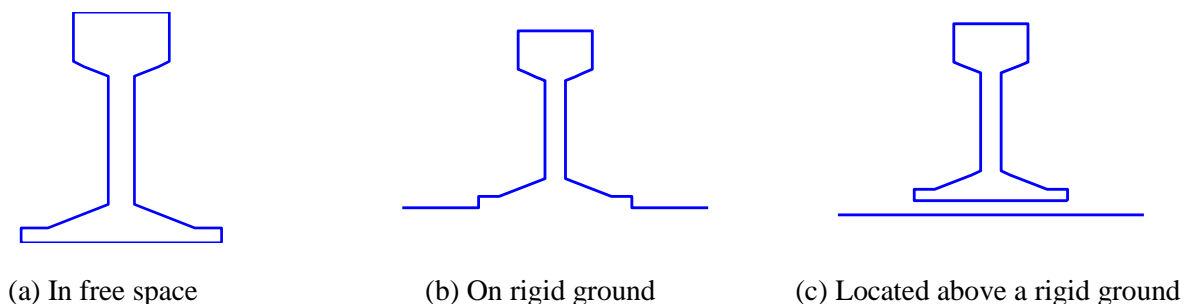


Figure 1. Two-dimensional Boundary Element models of a rail

Figure 2 shows the prediction of the sound radiation from the rail for the three cases. Specifically, Figure 2(a) shows the sound radiation from the rail for vertical motion. As can be seen, the radiation ratio of the rail in free space is proportional to f^3 at low frequency, which is characteristic of a line dipole. Above around 1 kHz the radiation ratio exhibits peaks and dips, which are due to the shape of the rail. Constructive and destructive interference between the sound radiation from the rail head and the rail foot cause these fluctuations in the radiation ratio. Taking the dip at 1 kHz, for example, the distance between the centre of the rail head and the rail foot is approximately half the acoustic wavelength at this frequency. Thus a dip occurs at this frequency because of destructive effects.

When it is located above the rigid ground, the dipole source will be reflected by the ground plane, so that a line quadrupole will be formed by the source and its image. This gives a slope proportional to f^5 at low frequency. It also can be seen a peak occurs at 850 Hz. At this frequency the acoustic wavelength is equal to 0.4 m which is twice the distance between the centre of the rail and its image source; hence at this frequency the two dipoles reinforce rather than forming a quadrupole. For the model of the rail attached to the rigid ground, the bottom of the rail foot cannot radiate sound, which means that the top and the bottom areas of the rail section are not equal. A net line monopole is present and the radiation ratio is proportional to f at low frequency. At high frequencies the results are similar for all three cases.

Figure 2(b) shows the corresponding results when the rail vibrates horizontally. At high frequencies, the radiation ratio tends to unity, although different peaks and dips again occur for the three cases due to the constructive and destructive interference effects of the different parts of the rail. Moreover, at low frequencies the calculated radiation ratios of these three models have the same slope, which is approximately proportional to f^3 . Therefore, when the rail moves laterally, the rail source can be treated as a line dipole for all three cases. However, in the presence of the rigid ground the effective size of the dipole is increased, shifting the transition frequency downwards and increasing the radiation ratio at low frequencies.

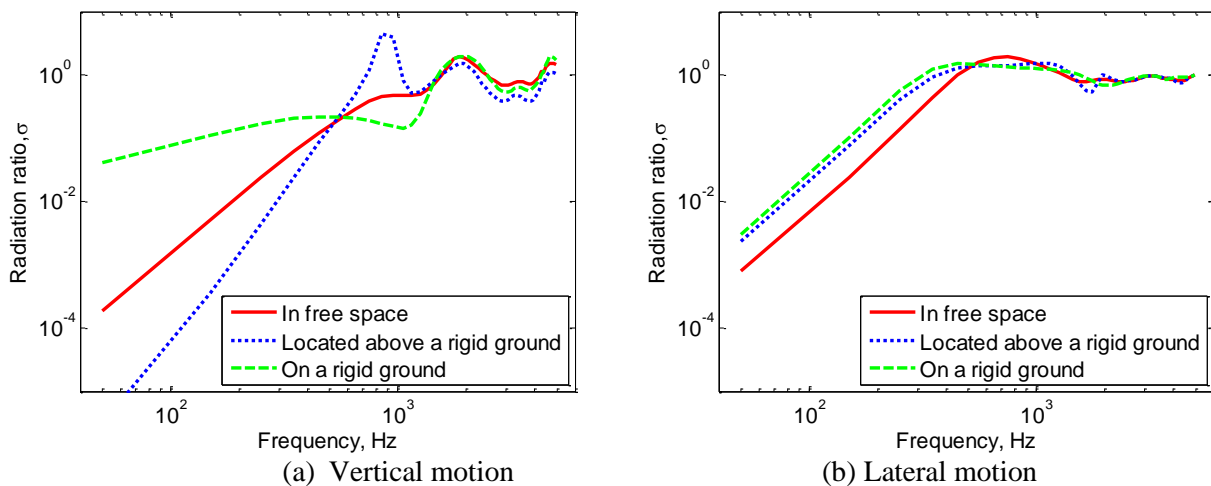


Figure 2. Sound radiation of the rail calculated for free space and in presence of a rigid ground

3. Sound radiation of the rail with an absorptive ground

In practice, the ground is not rigid, but has absorptive properties which can be described by the ground impedance. For engineering outdoor sound propagation problems, a simple and widely used model for ground impedance is that originally proposed by Delany and Bazley⁹ for porous materials. This model only depends on a single parameter, the flow resistivity. For ground, an equivalent value of flow resistivity can be selected by comparison with a measured impedance. Introducing this model for the impedance of the surface of the ground into the boundary element simulations, the results obtained are shown in Figure 3 for vertical and lateral motion. Results are shown for three values of flow resistivity, in each case for an infinite layer of absorptive material. The lower values of flow resistivity correspond to more absorptive ground.

It can be seen in Figure 3(a) that a more absorptive ground causes the rail to radiate more noise at low frequency. This is because the absorptive ground partly destroys the cancellation present for a reflective ground which led to the formation of a quadrupole source. At high frequency, however, particularly between 600 and 2000 Hz, the absorptive ground causes a reduction in the

sound radiation of the rail. On the other hand, for horizontal motion, when the ground becomes more absorptive the rail will radiate less noise over the whole frequency range, especially between 200 and 1000 Hz.

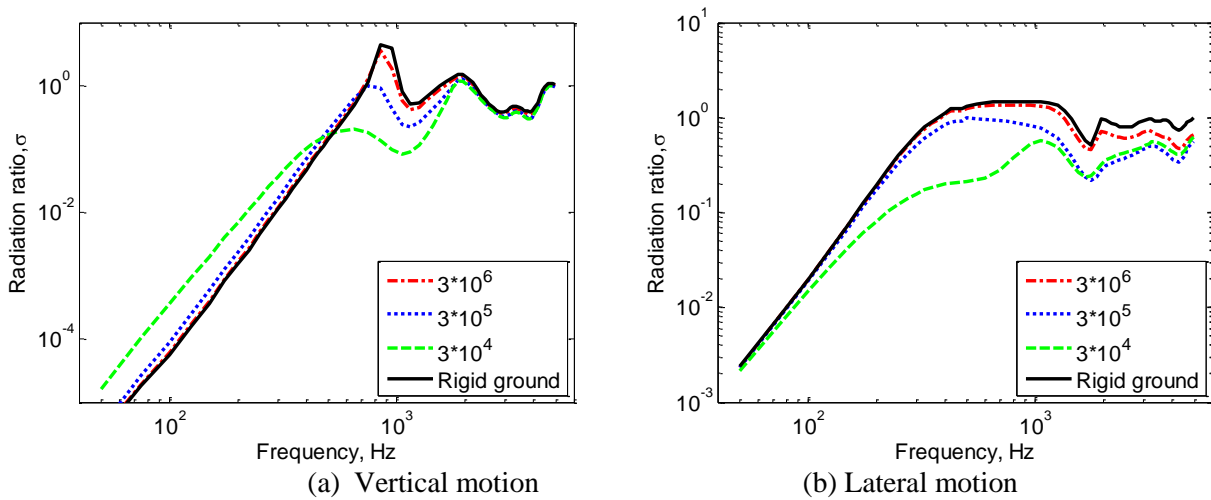


Figure 3. Sound radiation of the rail located 0.02 m above an absorptive ground with different values of flow resistivity

4. Experimental validation

Measurements have been carried out to investigate the sound radiation of a railway track. For these experiments, a 1/5 scale model of a railway track has been constructed, as shown in Figure 4. It has a length of 2 m. By testing at 1/5 scale, the frequencies are increased by a factor of 5 compared with full scale. The rails are commercially available steel rails used for miniature railways and are approximately 1/5 scale replicas of the UIC 60 section. Concrete sleepers have been specially constructed and 1/5 scale ballast has been obtained. However, the tests described here only used the rails. A constrained layer damping treatment has been applied to the bottom of the rail foot. This makes the damping ratio of the scaled rail more realistic and simplifies testing. Overall, the damping treatment increases the damping ratio to an average value of around 0.013. With this increased damping the frequency response of the rail shows less pronounced peaks, which makes the measurement procedure clearer (see below).



Figure 4. 1/5 scale model set up

Results are presented below for the rail in free space, above a rigid ground and above an absorptive ground. For the case of the rail on a rigid ground, however, it was not possible to realize the boundary conditions to allow verification of the model. Moreover, it is necessary to determine the critical frequency of the scaled rail (at which the bending and acoustic wavelengths are equal). For vertical motion, it can be calculated as 287 Hz, whereas it is 641 Hz for horizontal motion.

To obtain the rail radiation ratio experimentally, equation (1) can be written as

$$\sigma = \frac{W/\overline{F^2}}{\rho_0 c_0 \sum \left| \frac{v_i}{F} \right|^2 dS_i} \quad (2)$$

where $W/\overline{F^2}$ is the sound power normalised by the mean-square force and $|v_i/F|^2$ is the squared mobility from the force position to response position i . dS_i is the surface area of the rail associated with position i .

According to equation (2), two tests are required. One is to measure the transfer mobility, which has been carried out using an impact hammer. The other is to obtain the sound power for a given force. This has been determined reciprocally by measuring the acceleration response to a measured sound pressure field in a reverberation chamber.

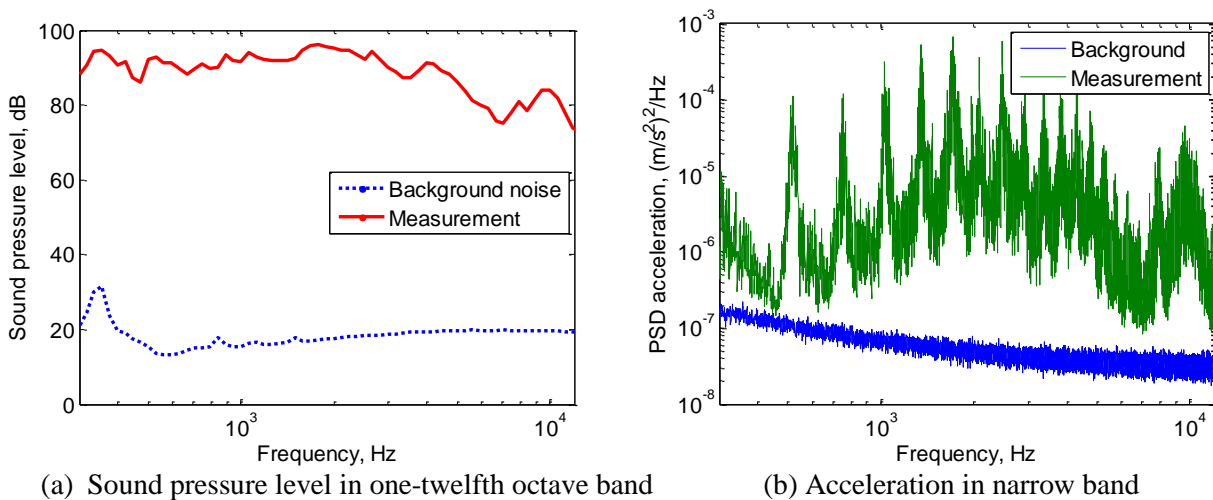


Figure 5. Comparison of measurement and background noise signals for rail in reverberation chamber

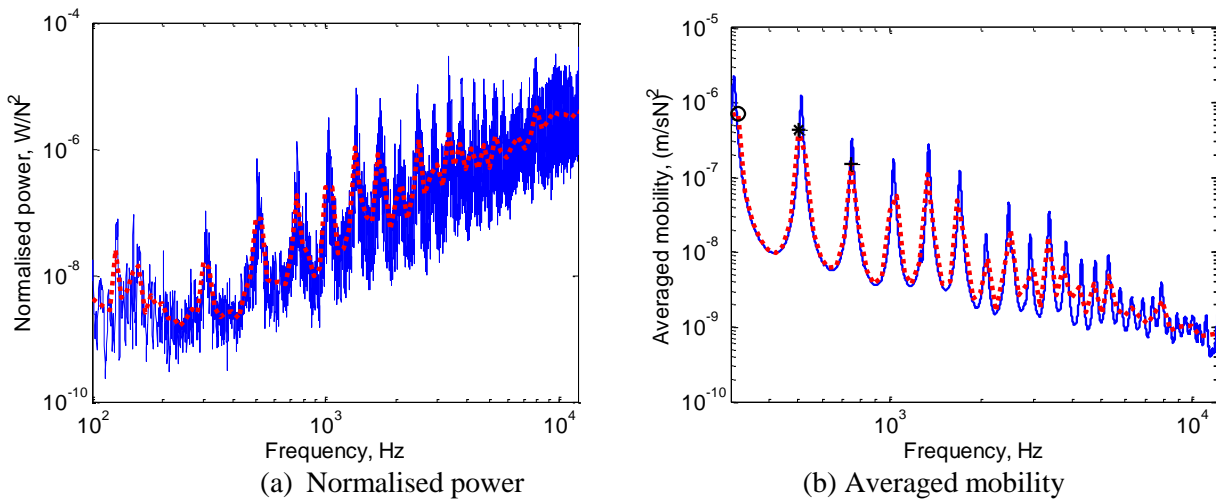


Figure 6. Normalised sound power and averaged mobility of rail in free space for vertical motion

A comparison of the measured sound pressure level with the background noise in the reverberation chamber is shown in Figure 5(a). Figure 5(b) shows equivalent results for the vertical acceleration signal. As can be seen, an adequate signal-to-noise ratio is achieved for the sound pressure, and at most frequencies for the acceleration. Figure 6(a) presents the normalised power obtained by the reciprocity method. The transfer mobility of the rail is shown in Figure 6(b). To smoothen the fluctuations seen in figure 5(b) and 6(a), subsequent results are averaged into one-twelfth octave bands.

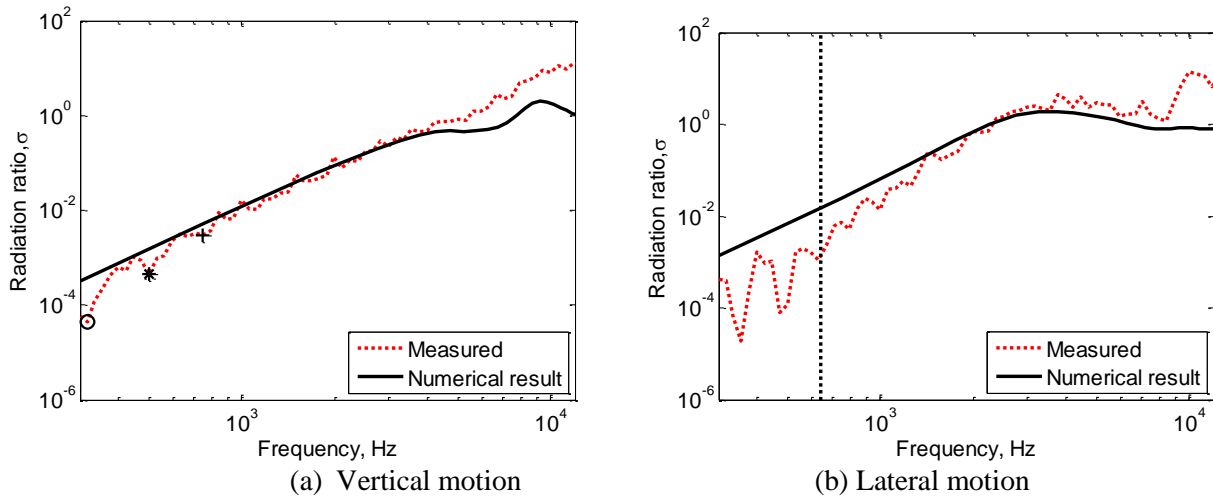


Figure 7. Comparison of numerical results and measurements for 1/5 scale rail in free space (the critical frequency is marked by a vertical line)

Figure 7(a) compares the numerical results and measurements for vertical motion of the rail in free space. It can be seen that the measurement curve has some peaks and dips between 300 Hz and 900 Hz, not found in the numerical result. The dips, marked as specific points, correspond to modes of the rail, as also indicated in Figure 6(b). Clearly the acoustic behaviour of low frequency modes can differ from that of the simple line dipole even above the critical frequency. In the frequency range 900 Hz~4 kHz, the experimental results agree very well with the numerical prediction. However, the measurement results are larger than numerical ones above 4 kHz, probably because of the influence of cross-sectional deformation of the rail which occurs at high frequency, whereas the predictions are based on a rigid vertical motion.

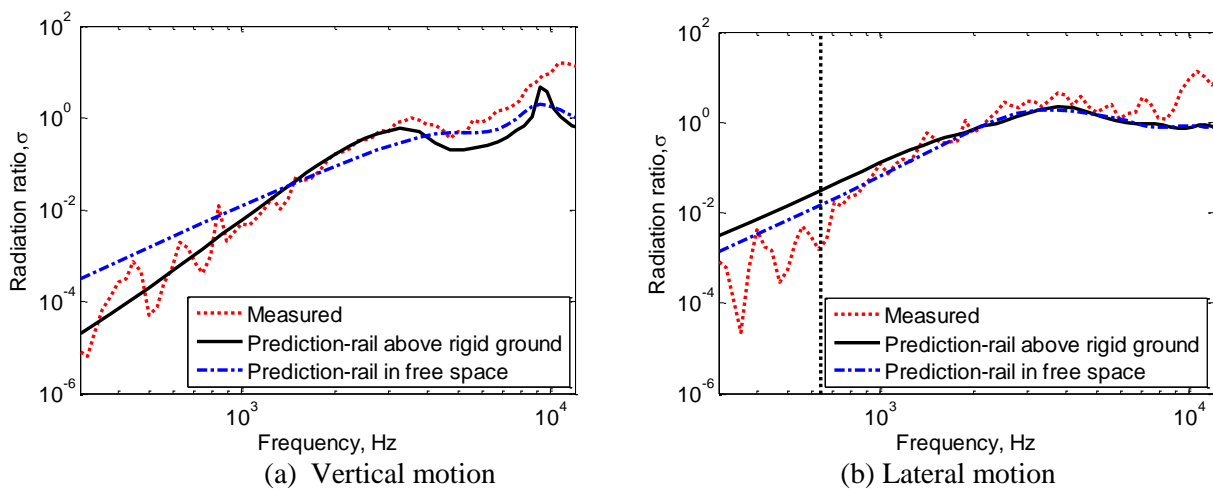


Figure 8. Comparison of numerical results and measurements for 1/5 scale rail 20 mm above rigid ground

For the rail with horizontal motion in free space in Figure 7(b), the experimental results are lower than the prediction below the critical frequency, due to the acoustic short-circuiting. Above the critical frequency, it can be seen the measured results agree reasonably well with the numerical results. However, the experimental results are larger than the numerical results above around 3 kHz. This may again be because of the effects of the cross-section deformation of the rail.

The effects of the rigid ground on the sound radiation of the rail are presented in Figure 8. The predicted results for the rail in free space are shown for comparison. For vertical vibration, the measured result agrees very well with the boundary element calculations up to approximately 3 kHz. Above this frequency, the measured radiation ratio is again larger than the prediction but the change relative to the free space result is correctly predicted. The experimental results again show dips at the frequencies of the vibration modes below 1 kHz.

For horizontal motion, the measured radiation ratio agrees with the boundary element prediction very well between approximately 1 and 8 kHz, as shown in Figure 8(b). Again the measured results are lower than the corresponding boundary element calculations below the critical frequency.

In order to test the case of the rail above an absorptive ground, the rail was measured above a piece of melamine foam, with dimensions 2 m × 0.4 m × 50 mm. Its impedance was measured in an impedance tube and the corresponding flow resistivity was obtained as 12000 Pa.s/m² by fitting the Delany-Bazley model to this measurement. A comparison of the measurements with the numerical calculations is shown in Figures 9(a) and (b).

Figure 9(a) compares the measurement with the prediction for vertical motion. The agreement is very good, except at very high frequency. For horizontal motion, Figure 9(b) shows very good agreement between the predicted and the measured data between 800 and 8000 Hz.

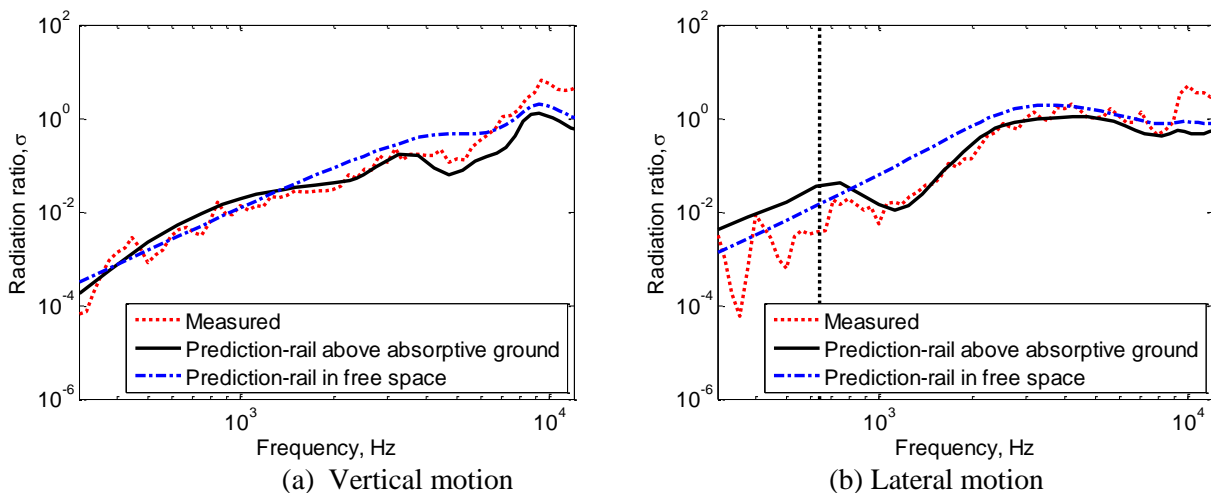


Figure 9. Comparison of numerical results and measurements for 1/5 scale rail 20 mm above absorptive ground

5. Conclusions

The influence of the ground impedance on the rail radiation is presented in this paper. Using a two-dimensional boundary element model, it has been found that the radiation has the properties of a line dipole for a rail in free space. For vertical motion above a rigid ground this is changed to that of a line quadrupole, while it becomes a line monopole when the rail is attached to the rigid ground. For horizontal vibration of the rail, however, the radiation follows the characteristics of a line dipole for all three cases. Furthermore, it has been shown that the ground absorption will reduce the sound

radiated by the rail for lateral motion over the whole frequency range. For the rail vibrating vertically, however, an absorptive ground will make the rail radiate more noise at low frequency, whereas the rail radiation will be decreased at higher frequencies.

Corresponding measurements have been performed on a scale model to verify the numerical prediction for the rail in different configurations. For both vertical and lateral vibration, the agreements between the measured results and numerical predictions have been shown to be very good for the rail in all configurations. In general, however, the measured radiation ratio is somewhat greater than the numerical estimates at high frequency, which is probably due to the presence of cross-section deformation. Moreover, for lateral motion, the boundary element models overestimate the rail radiation ratio below the critical frequency of the rail because of the acoustic short-circuiting.

Acknowledgments

The work described has been supported by the EPSRC under the programme grant EP/H044949/1, 'Railway Track for the 21st Century' and by the EU project ACOUTRAIN, Virtual certification of acoustic performance for freight and passenger trains, collaborative project number 284877 funded under the Seventh Framework.

REFERENCES

- ¹ Thompson, D.J. Predictions of acoustic radiation from vibrating wheels and rails. *Journal of Sound and Vibration*, **120** (2), 275-280, (1988).
- ² Nilsson, C.-M, Jones, C.J.C, Thompson, D.J. and Ryue, J. A waveguide finite element and boundary element approach to calculating the sound radiated by railway and tram rails. *Journal of Sound and Vibration*, **321** (3-5), 813-836, (2009).
- ³ Bender, E.K, Remington, P.J. The influence of rails on train noise. *Journal of Sound and Vibration*, **37** (3), 321-334, (1974).
- ⁴ Remington, P.J. Wheel/rail noise—Part I: characterization of the wheel/rail dynamic system. *Journal of Sound and Vibration*, **46** (3), 359-379, (1976).
- ⁵ Remington, P.J. Wheel/rail rolling noise I: theoretical analysis. *Journal of the Acoustical Society of America*, **81** (6), 1805-1823, (1987).
- ⁶ Chessell, C.I. Propagation of noise along a finite impedance boundary. *Journal of the Acoustical Society of America*, **62**, 825-834, (1977).
- ⁷ Thompson, D.J., Hemsworth, B., Vincent, N. Experimental validation of the TWINS prediction programme for rolling noise, Part 1: Description of the model and method. *Journal of Sound and Vibration*, **193** (1), 123-35, (1996).
- ⁸ Thompson, D.J., Jones, C.J.C., Turner, N. Investigation into the validity of two-dimensional models for sound radiation from waves in rails. *Journal of Acoustical Society of America*, **113** (4), 1965-1974, (2003).
- ⁹ Delany, M.E., Bazley, E.N. Acoustical properties of fibrous absorbent materials. *Applied Acoustics*, **3** (2), 105-116, (1970).